Stark broadening of spectral lines along the isoelectronic sequence of Li

S. Glenzer, N. I. Uzelac,* and H.-J. Kunze
Institut für Experimentalphysik V, Ruhr-Universität, 4630 Bochum, Federal Republic of Germany
(Received 13 January 1992)

Experimental Stark widths of the $3s\,^2S - 3p\,^2P^\circ$ transitions in the Li-like ions C IV, N V, O VI, and Ne VIII are reported. The measurements were performed for a set of plasma parameters so that the density and temperature behavior of the Stark widths could be observed and compared with calculations. The experimental results did not show a scaling with Z^{-2}, where Z is the spectroscopic charge number, which is expected from theoretical calculations in the electron-impact approximation. Furthermore, deviations from linear scaling appear for $Z = 8$.

PACS number(s): 52.70.Kz, 32.70.Jz

I. INTRODUCTION

Investigations of Stark widths of highly charged nonhydrogenic ions along isoelectronic sequences are of great interest since cross sections for impact broadening scale with nuclear charge and therefore systematic trends for Stark widths are expected. For checking the predictions of modern theories of Stark broadening reliable measurements are essential, and they would also allow the extrapolation of widths to higher ionization stages.

Up to now most measurements are restricted to a sequence of at most three elements (see, e.g., Refs. [1–3]) and low charges (up to $Z = 4$). The agreement between theoretical approaches and available experimental data is such that no definite answer could be given as to what the scaling of widths with Z actually is.

The only measurements in well-diagnosed plasmas involving highly ionized atoms ($Z > 4$) were recently performed by Böttcher *et al.* [4]. Their results of the Stark widths of Li-like $3s\,^2S_{1/2} - 3p\,^2P^\circ_{3/2}$ transitions of C IV, N V, and O VI indicated a Z^{-1} dependence contrary to the above-mentioned calculations giving nearly a Z^{-2} dependence.

In an attempt to solve the questions raised, we carried out new measurements of Stark broadened profiles using the same gas-liner pinch as Böttcher *et al.* [4]. After improving the device, its operation, and the diagnostic procedures, we recorded the profiles of the same lines of C IV, N V, and O VI as in Ref. [4] but also extended the observed isoelectronic sequence to higher Z by measuring the Ne VIII $3s\,^2S - 3p\,^2P^\circ$ lines at 282.07 and 286.01 nm.

The experimental results are compared with theoretical widths, which we calculated according to Refs. [5] and [6], and with recent improved calculations by Hey [9].

Apart from the scaling of Stark widths with Z an attempt was made to investigate scaling with electron temperature and density for each of the lines under investigation.

It should be mentioned that data for Stark broadening of highly ionized systems are also required to describe the radiative transport in stellar interiors (see, e.g., Ref. [5]).

II. THEORETICAL STARK WIDTHS

For the calculation of the Stark widths we choose the semiclassical impact theory of Ref. [5] and a modified semiempirical approach as given in Ref. [6]. Applying Eq. (526) of Ref. [5] Bates-Damgaard factors were introduced and effective principal quantum numbers were used. They also were used in Eqs. (7) to (9) of Ref. [6], whereby the Gaunt factors were interpolated from the values given in the same reference. The Bates-Damgaard factors were taken from Ref. [7] and data for energy levels from Ref. [8].

Calculations of the electron-impact broadening were also performed by Hey [9], who used the semiclassical Gaunt-factor approximation. He introduced some improvements in the calculation of the strong collision contributions (whereby both the disruptive and higher-multipole collisions are included) to the broadening along the lines indicated in Ref. [10], and improved the method of averaging over the strong collisions. The assumptions were made that the electron-radiator collisions are the dominant broadening mechanism, and that the impact approximation of Baranger [11] remains valid [12] for the electron densities and temperatures of the present experiment [13].

Although ion broadening through the quadratic Stark effect is negligible, broadening through quadrupole interactions is typically of the order of 10% of the impact width [Eq. (218a) of Ref. [5]]. For higher temperatures, however, its relative contribution becomes larger, since it is approximately independent of temperature.

III. EXPERIMENT

A. Plasma source

The measurements of the line profiles were carried out on the gas-liner pinch device developed at Ruhr-Universität Bochum [14–16]. It resembles a large aspect ratio Z pinch where the so-called driver gas (in our case hydrogen) is injected through a fast-acting electromagnetic valve with an annular nozzle, forming initially a hollow gas cylinder near the wall. After preionization (a

50-nF capacitor charged to 20 kV is discharged through 50 annularly mounted needles) a 11.1-μF capacitor bank (25–35 kV) is discharged through the initial plasma shell resulting in a compressed plasma column 1–2 cm in diameter and 5 cm in length.

Another fast valve independently injects the test gas, in our case CH_4, N_2, CO_2, or Ne, along the axis of the discharge tube. If this injection is properly timed, the ions of the test gas remain concentrated in the central part of the discharge where the plasma is rather homogeneous. In this way cold boundary layers of the gas under investigation are absent, as has been verified experimentally (see below).

The implosion time of the discharge and the lifetime of the plasma were about 2.7 and 0.5 μs, respectively. The maximum current reached was about 380 kA, and the plasma parameters in the center of the discharge were between $1.0 < n_e < 2.9 \times 10^{18}$ cm^{-3} and $7.0 < kT_e < 42.5$ eV. For this range of plasma parameters no self-absorption of investigated lines was detected, as will be discussed later. Several discharge conditions were used for the different ionic species.

These features of the plasma source critically depend on the amount of the test gas and its injection during the time of plasma generation, and when set properly, make the gas-liner pinch an important, very suitable source for line-broadening studies at high electron densities.

B. Plasma spectroscopy

The experimental setup is shown in Ref. [17], and only a few details are given here. The radiation from the discharge is observed side-on through a port in the chamber and imaged onto the entrance slit (30 μm wide) of a 1-m monochromator (Spex model 1704) with 1:1 magnification and $f/12$ collection optics. In the exit plane of the monochromator an optical multichannel analyzer (OMA II) detector head was mounted, operating in the pulse mode with a gate duration of 30 ns. Using a 1200-lines/mm plane grating blazed at the wavelength of 500 nm, the linear reciprocal dispersion was 0.0201 nm/pixel in the first order, which was used for recording the C IV spectral lines.

A higher resolution was needed for the other lines, since the Stark widths decrease with increasing Z. For the investigation of the N V, O VI, and Ne VIII lines we employed, therefore, a grating with 1200 lines/mm, blazed at 1000 nm. Using it in second, third, and fourth orders, the linear reciprocal dispersions were 0.0090, 0.0055, and 0.0043 nm/pixel in the respective wavelength ranges. Contributions to the line profiles from other orders could be eliminated by proper filters (GG385, UG5, and glass).

When recording the Ne VIII $\lambda = 282.07$-nm line, it was not possible to isolate the fourth-order radiation, but fortunately, there was no line radiation from the third order, which could not be removed using filters. The fourth-order Ne VIII multiplet lines are separated in wavelength such that the lines could not be recorded simultaneously with the OMA. In order to check their intensity ratio, we also measured this doublet in first order employing a 2400-lines/mm plane grating blazed at 240 nm, yielding a linear reciprocal dispersion of 0.0102 nm/pixel.

The pixel-to-pixel sensitivity calibration of the detection system was obtained for each wavelength range under investigation using a standard tungsten lamp, smoothing the averaged recorded spectra by the procedure of adaptive smoothing [18]. The wavelength calibration was done with the aid of He and Ne spectral lamps and with Fe and Al hollow cathode lamps. The recorded apparatus profile of the detection system had a full width at half maximum (FWHM) of 4–5 pixels. Its contribution to the recorded profile was taken into account, as will be shown later.

The reproducibility of the discharge was tested by monitoring the plasma continuum radiation at 520 nm with a photomultiplier mounted at the exit slit of a $\frac{1}{4}$-m monochromator. This signal was also used to control the gating time settings of the OMA and the laser for different phases of the discharge.

C. Plasma diagnostics

Electron densities and ion temperatures at the center of the plasma were determined by 90° Thomson scattering [19]. The evaluation procedure was improved by taking into account effects on the scattering spectra caused by the impurity ions [20]; details are discussed by DeSilva *et al.* [21]. This procedure yields the electron density n_e, ion and electron temperatures (T_i and T_e), and the temperature and concentration of impurity ions (T_{imp} and n_{imp}), if the mean charge $\overline{Z}$ of the impurity ions is determined independently. We therefore derived $\overline{Z}$ by observing lines from successive ionization stages.

The analysis of the Thomson scattering spectra yielded the following results: $T_i = T_e$ within the error limits for all plasma conditions investigated. The impurity ion temperature T_{imp} was found to be slightly higher than the electron temperature T_e, but still within the error limits; this can be expected when one compares the time scale of equilibration between impurity ions and protons [22] with the plasma implosion time. The impurity ion concentration n_{imp} was determined to be about or less than 1% of the electron density n_e.

We could also verify from the shapes of the spectra that there were no macroscopic plasma turbulences, instabilities, or relative drifts of the ions and electrons occurring during the times of observation, which had **k** vectors in the plane perpendicular to the discharge axis. Thomson scattering was performed using a Korad Q-switch-driven ruby laser (K-1Q) giving a 2.5-J, 20-ns pulse. The resulting spectra were recorded with the detection system described above, using a 1200-lines/mm grating in second order (the linear reciprocal dispersion was 0.0063 nm/pixel). This allowed us to resolve the impurity peak of the scattering spectra.

IV. RESULTS AND DISCUSSION

Line profiles were obtained for different combinations of plasma parameters simply by recording the spectra at

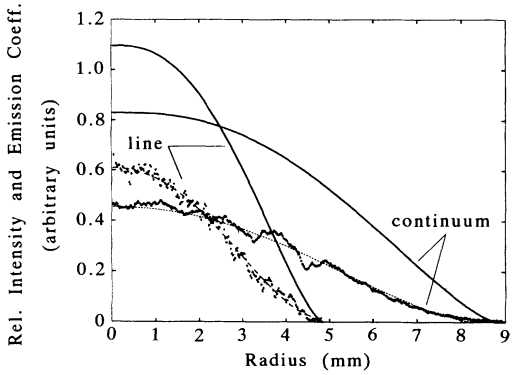

FIG. 1. Radial distribution of line and continuum radiation as emitted from the gas-liner pinch plasma about 200 ns after maximum pinch compression. ···, recorded intensities; —, corresponding radial emission coefficients obtained as Abel inversions of polynomial fits (- - -) to those intensities.

different times during the discharge, starting at the time of maximum compression, and observing the emission in the decay phase of the plasma as long as the plasma could be considered homogeneous in density and temperature over that volume from which the test-gas ions emit.

This was checked by recording and comparing continuum emission and line intensities over the cross section of the plasma column. For this purpose the cross section of the plasma was imaged onto the entrance slit of the monochromator, the intensity distribution along the height of the exit slit thus reflecting directly the radial intensity distribution of the plasma column in the respective wavelength interval. This intensity distribution was conveniently recorded with an OMA system, the diode array also aligned along the height of the exit slit. Figure 1 shows an example of the radial distribution of line and continuum emission as well as local emission coefficients as obtained after Abel inversion. These emission coefficients confirm that the test-gas ions indeed are confined to the center of the plasma column and effectively emit from a practically homogeneous plasma only. The continuum radiation is proportional to $n_e^2/\sqrt{T_e}$ [23], and it follows that the electron density changes by less than 10% over the plasma volume from which more than 95% of the line radiation is emitted. The errors introduced by assuming a homogeneous plasma in the data evaluation thus will be less than 3% in the Stark widths. The radial emission was further checked as a function of time and showed that conditions as above suitable for our measurements prevailed up to at least to 200 ns after maximum pinch compression.

Two additional constraints limited the range of plasma parameters for which spectra were recorded. The lines under investigation ought to be isolated from other lines with an acceptable signal-to-noise ratio, and the observations were preferably carried out only during stages of the discharge with smooth changes in the plasma parameters.

The monitor signal was used to select identical plasma

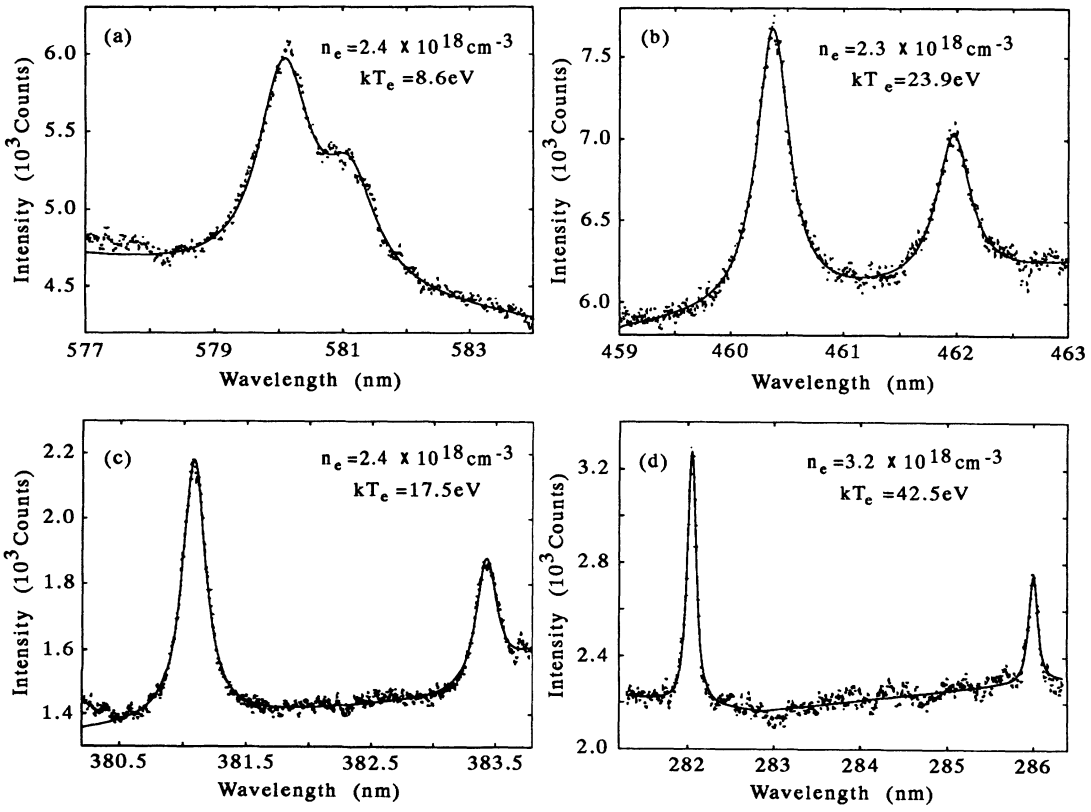

FIG. 2. Examples of recorded line spectra of $3s\ ^2S - 3p\ ^2P^\circ$ transitions; ···, recorded; —, Voigt function best fit. (a) C IV, (b) N V, (c) O VI, and (d) Ne VIII. Electron densities and temperatures are from Thomson scattering.

conditions, and about eight line profiles were averaged to reduce noise. The profiles were fitted by a Voigt function employing a least-squares fitting procedure [24]. The Voigt function was the convolution of the measured apparatus profile, a Doppler profile calculated for the measured ion temperature, and a Lorentz function with variable width for the Stark broadening. The fitting procedure also included variation of the continuum. Figure 2 shows examples of profiles of recorded spectral lines along with their fits. It should be noted here that the contribution of Doppler broadening to the overall width of the spectral lines under investigation did not exceed 15%, that of the apparatus profile being less than 12%.

The multiplet components were fitted by two independent Lorentzian profiles (Fig. 2). For all our profiles the shape of the continuum in the wavelength range under consideration was assumed to be linear, which was confirmed by recording respective spectra of discharges without injection of test gas.

Line-broadening mechanisms other than those mentioned above could be neglected for the lines and the range of plasma parameters under investigation. Despite the high discharge current, even the effect of Zeeman splitting was found to be negligible; it was calculated according to Ref. [25] for our measured magnetic induction **B**. The magnitude of **B** inside the plasma column was eight times smaller than outside the plasma; this was obtained from measurements with magnetic probes [26] and verified by measuring the discharge current with a Rogowski coil and estimating **B** using magnetohydrodynamic equations.

The recorded spectra (Fig. 2) showed that distortions of the profiles due to opacity effects (self-absorption) were absent. For each species, the intensity ratio of the two multiplet components was found to be 2:1 with fair accuracy; in the case of self-absorption it would have been smaller. For C IV, where the doublet components overlap due to Stark broadening, we checked the intensity ratio of the $2s\ ^2S_{1/2} - 2p\ ^2P^o_{3/2}$ and $2s\ ^2S_{1/2} - 2p\ ^2P^o_{1/2}$ resonance lines in the vacuum ultraviolet, which are less broadened: it was also 2:1. This assures that the $3s - 3p$ lines in the visible were indeed optically thin.

Table I gives the experimental Stark widths (FWHM) and the measured electron density and temperatures. The errors are estimated rms values from individual spectra. The largest contribution to the error is due to shot-to-shot irreproducibility, which is rather good for such experiments (note, the estimated errors are not greater than 25%). The last three columns contain theoretical widths, which were calculated after Refs. [5] and [6] or were made available [9].

The Stark widths from the recorded spectra (Fig. 2) were the same for both $3s\ ^2S_{1/2} - 3p\ ^2P^o_{3/2}$ and $3s\ ^2S_{1/2} - 3p\ ^2P^o_{1/2}$ components within the error limits; however, the values given in Table I were determined only from the more intense lines for their better signal-to-noise ratio. In case of Ne VIII, the Stark widths were taken from spectra of the $3s\ ^2S_{1/2} - 3p\ ^2P^o_{3/2}$ transiton with higher resolution.

In order to compare our experimentally determined Stark widths with those obtained from theoretical approaches [5, 6, 9] and from other experiments [4, 27–30], the widths were plotted as functions of electron temperature and density in Figs. 3 and 4. Since the only available experimental result for higher ionization stages (Ref. [4]) is obtained for $n_e = 1.8 \times 10^{18}$ cm^{-3} and $kT_e = 12.5$ eV, our results are scaled to these plasma parameters for a better comparison. A linear scaling of Stark widths with electron density was assumed for plotting the data in Fig. 3, since the linear dependence of Stark widths of spectral lines of isolated nonhydrogenic ions upon electron density has been checked and proven in numerous experiments (see, e.g., Refs. [3, 5, 31, 32]).

However, because the temperature in our experiment had to be increased appreciably (by increasing the discharge voltage) to obtain the desired ionization stage of the heavier elements, it was essential to study first the temperature dependence of the Stark widths for each measured line, in order to compare them to those obtained at lower temperatures.

The assumption of a constant Gaunt factor results in a

TABLE I. Experimental Stark widths w_m of investigated $3s\ ^2S_{1/2} - 3p\ ^2P^o_{3/2}$ transitions in Li-like ions. Experimental results are compared with theoretical widths w_G calculated after Ref. [5], w_{DK} after Ref. [6], and w_H calculated in Ref. [9]

Ion	λ (nm)	kT_e (eV)	n_e (10^{18}cm^{-3})	w_m (nm)	w_m/w_G	w_m/w_{DK}	w_m/w_H
C IV	580.13	7.0 ± 0.7	1.5 ± 0.3	0.67 ± 0.04	0.90	1.19	1.19
		8.6 ± 0.8	2.4 ± 0.2	0.97 ± 0.05	0.88	1.15	1.14
N V	460.37	14.9 ± 2.3	1.2 ± 0.2	0.22 ± 0.01	1.18	1.51	1.37
		18.7 ± 4.0	1.6 ± 0.3	0.27 ± 0.01	1.12	1.40	1.29
		21.8 ± 5.3	2.0 ± 0.4	0.34 ± 0.02	1.10	1.39	1.26
		23.9 ± 5.6	2.3 ± 0.4	0.38 ± 0.02	1.12	1.42	1.28
O VI	381.13	8.3 ± 2.3	1.0 ± 0.2	0.10 ± 0.01	1.21	1.42	1.28
		11.5 ± 2.1	1.3 ± 0.3	0.14 ± 0.01	1.38	1.64	1.44
		15.6 ± 3.5	2.1 ± 0.4	0.18 ± 0.03	1.16	1.37	1.21
		17.5 ± 1.9	2.4 ± 0.3	0.21 ± 0.02	1.26	1.50	1.32
Ne VIII	282.07	29.7 ± 7.1	2.8 ± 0.3	0.12 ± 0.01	2.22	2.55	1.83
		42.5 ± 11.4	3.2 ± 0.4	0.12 ± 0.01	2.07	2.45	1.77

$1/\sqrt{T_e}$ scaling of the impact widths [5, 6, 33]. For higher temperatures, however, the temperature dependence of the Gaunt factor itself competes with this scaling and impact widths become rather insensitive to temperature variations. As can be seen from Fig. 3, the theoretical approaches of Refs. [5] and [6] show a similar behavior of the FWHM with temperature but the values after [5] are systematically larger. The temperature dependence of the results of Ref. [9] is consistent with that mentioned above in the temperature range investigated in our experiment but the values are increasingly higher than those after [6] with higher Z. Our experimental results seem to support this trend. With the exception of C IV the values are systematically larger than the theoretical ones but confirm the predicted behavior of the Stark widths with temperature. However, at very high temperatures the scaling certainly should change due to the increasing importance of ion quadrupole broadening [5].

Our result is a very important finding since the agreement between most of the experimental data on the temperature dependence of Stark widths (as reviewed, e.g., by Konjević and Wiese [3]) and available theoretical results is poor. For example, the Stark widths of the resonance lines of Ca II measured in one experimental device (see Fig.1 of Ref. [3]) increase with temperature, in contrast to the theoretical expectations.

We now accepted the temperature dependence of the Stark widths as determined by the choice of effective Gaunt factors [6], and scaled all our measured values to a temperature of $kT_e = 12.5$ eV. These values are plotted in Fig. 4 as function of density together with theoretical calculations for this temperature. All experimental data show a linear dependence on the electron density as suggested by theories [5, 6, 9], but the values are higher than the theoretical ones (with exception of C IV), the difference increasing with Z.

Table I, finally, shows our measured Stark widths and theoretical ones calculated for the specific densities and temperatures. The values after Griem [5] and by Hey [9] match our data slightly better than those obtained after Dimitrijević and Konjević [6]. With the exception of Ne VIII, the values after Ref. [5] are closer to the experimental ones than those obtained in Ref. [9].

The experiment performed by Böttcher *et al.* [4] resulted in even higher Stark widths [see Figs. 3(a)–3(c) and 4(a)–4(c)] and attention should be drawn, therefore, to differences in the experimental procedures between that and the present experiment. One major difference is the improved diagnostics of the plasma introduced in the present work, where electron density and temperature were now derived for each discharge condition with the respective test-gas concentration, also taking into ac-

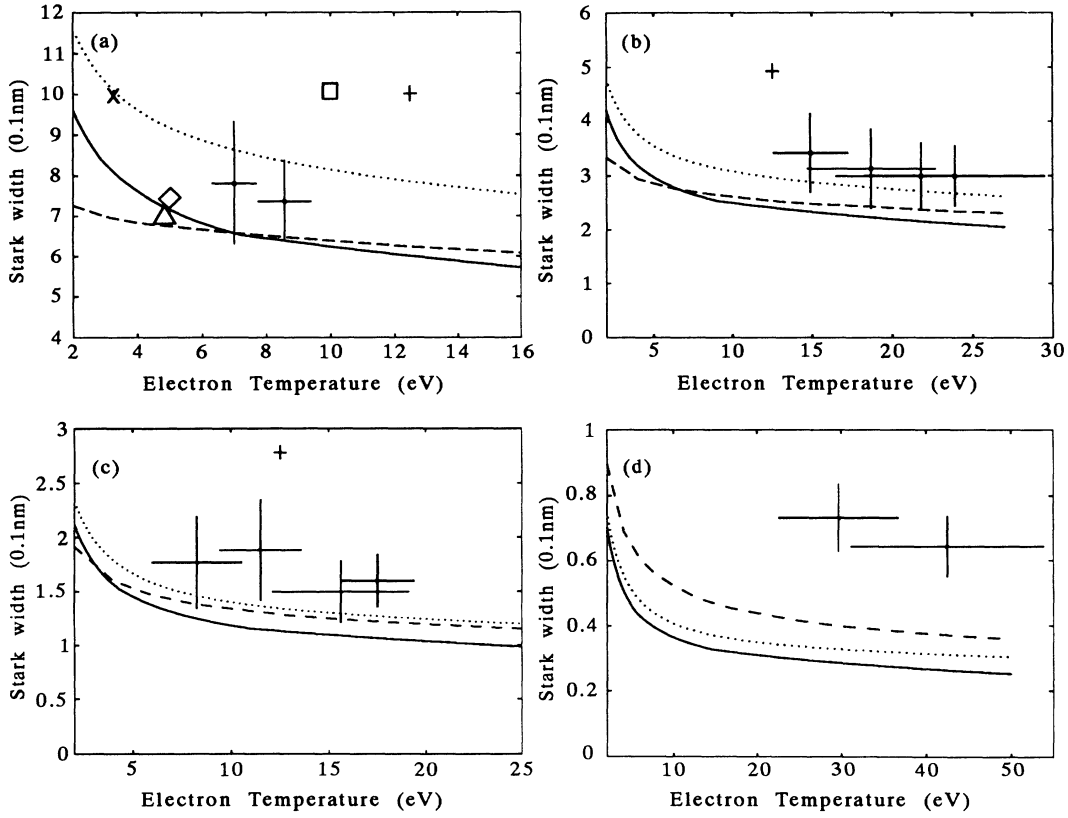

FIG. 3. Stark widths of the $3s\ ^2S - 3p\ ^2P^\circ$ doublet as a function of electron temperature for an electron density of $n_e = 1.8 \times 10^{18}\text{cm}^{-3}$. The experimental results (except [4]) are scaled to that density and calculations [5, 6, 9] are performed for that value of n_e. (a) C IV, (b) N V, (c) O VI, and (d) Ne VIII; ···, calculations after Ref. [5]; —, calculations after Ref. [6]; - - -, calculations by Ref. [9]. Experimental values: •, present experiment; +, Ref.[4]; □ , Ref. [27]; ◇ , Ref. [28]; △ , Ref. [29]; × , Ref. [30].

count the effects of the test-gas ions on the scattering spectra [21].

The neglect of the influence of even small amounts of test-gas ions could lead to underestimated electron densities and hence to Stark widths which are apparently too high. Another improvement was made in the procedure of fitting Voigt functions to the measured profiles (compare, e.g., Figs. 2(a)–2(c) with Fig.1 of Ref. [4]).

A comparison of measured and calculated Stark widths along the investigated isoelectronic sequence is given in Fig. 5. It should be noted that the error bars in Fig. 5 incorporate not only the error of the Stark-width determination but also the uncertainty in the electron-density and temperature measurements.

As can be seen from Fig. 5, the theoretical approaches of Refs. [5] and [6] show nearly a Z^{-2} dependence of the Stark width. The widths calculated by Seaton [34] using close-coupling theory coincide practically with those of Ref. [6]. The values calculated in Ref. [9] have roughly the same trend with somewhat higher values for higher Z.

Our experimental values for $Z > 4$ are systematically higher than the theoretical ones (see Table I), and do

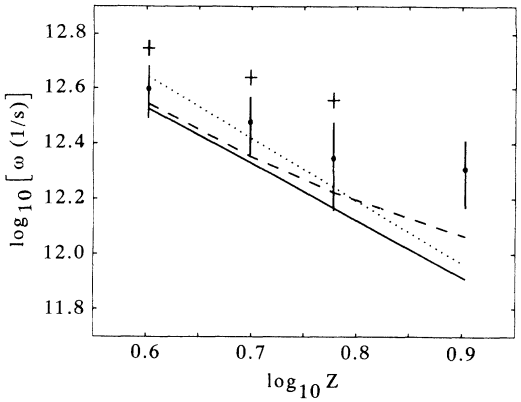

FIG. 5. Electron-impact Stark width w (in frequency units) of the transition $3s\ ^2S - 3p\ ^2P^\circ$ in C IV, N V, O VI, and Ne VIII vs the ion charge (expressed through the spectroscopic charge number Z): ···, calculations after Ref. [5]; —, calculations after Ref. [6]; - - -, calculations by Ref. [9]; experimental values: •, present experiment; +, Ref. [4]. The results of the present experiment are scaled to $n_e = 1.8 \times 10^{18}\text{cm}^{-3}$ and $kT_e = 12.5$ eV, and calculations [5, 6, 9] are performed for these values.

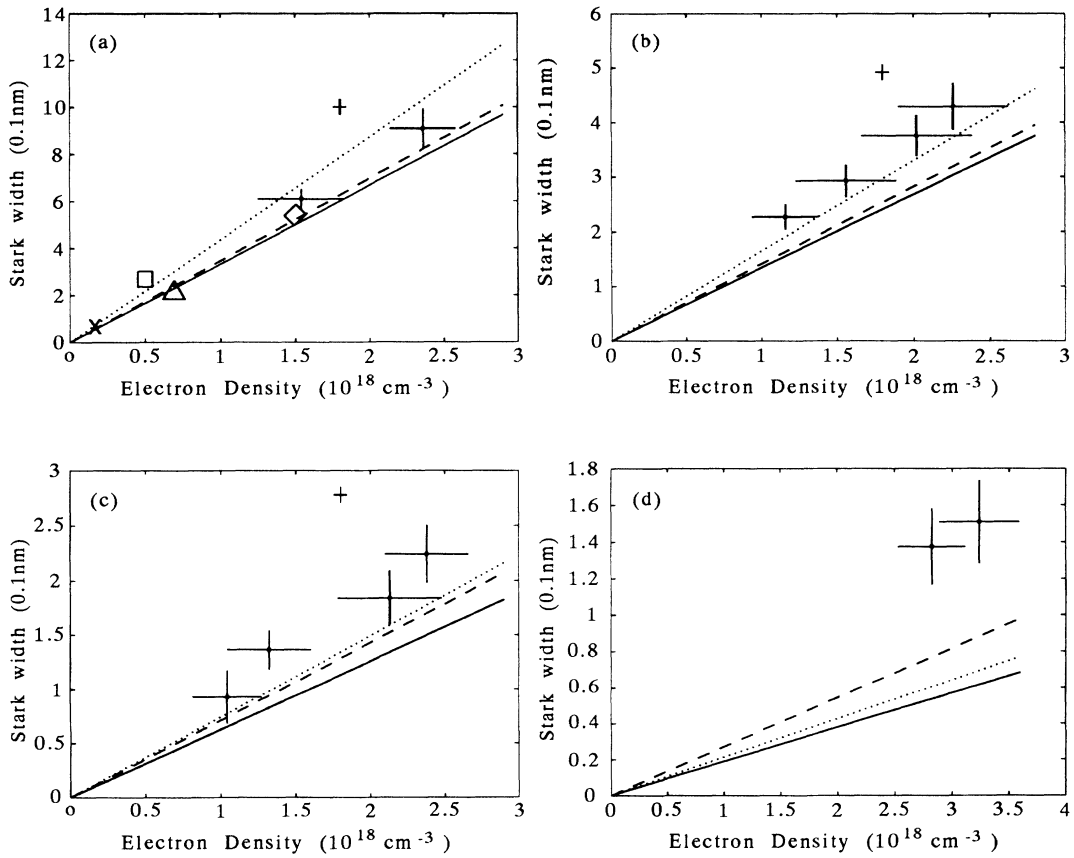

FIG. 4. Stark widths of the $3s\ ^2S - 3p\ ^2P^\circ$ doublet as a function of electron density for an electron temperature of $kT_e = 12.5$ eV. Experimental results (except [4]) are scaled to that temperature and calculations [5, 6, 9] are performed for that value of kT_e. (a) C IV, (b) N V, (c) O VI, and (d) Ne VIII; ···, calculations after Ref. [5]; —, calculations after Ref. [6]; - - -, calculations by Ref. [9]. Experimental values: •, present experiment; +, Ref. [4]; □ , Ref. [27]; ◇ , Ref. [28]; △ , Ref. [29]; × , Ref. [30].

not support the theoretical scaling. The value for $Z = 8$ is considerably larger if we extrapolate the widths from ionization stages $Z = 4$ to 6 to $Z = 8$. Calculations by Hey [9] show a similar tendency.

The scaling of all values to one temperature of 12.5 eV was done for the purpose of comparing the results, being aware of the facts that there will be no substantial Ne VIII population for observation at such low temperatures, and that for the temperatures of this experiment the ion quadrupole contribution, which has a different scaling, is at least 15%.

When comparing the results of the calculations [5, 6, 9] it should be noted that in Ref. [9], which is based on methods developed in Refs. [10, 12], some improvements in the calculation of the strong collision contributions to the broadening have been made, and that the method of averaging over the strong collisions was improved. This gives a strong collision contribution to the linewidth of about 20–25% for C IV, 25–30% for N V, 40–50% for O VI, and 50–60% for Ne VIII. In Ref. [6] no explicit expression for the strong collision contribution is given, but the disruptive collisions and higher multipole interactions in Ref. [5] were calculated to be between 12% and 14% of the linewidth for C IV to Ne VIII. The ion quadrupole broadening is poorly known, and the observed discrepancies will hopefully stimulate detailed calculations.

V. CONCLUSIONS

Measurements of Stark widths for the $3s\ ^2S - 3p\ ^2P^\circ$ transitions along the isoelectronic sequence of Li-like ions are reported for C IV, N V, O VI, and Ne VIII. Calculations after Refs. [5] and [6] are performed and compared with the experimental values along with the results supplied by Ref. [9]. All available experimental data of other authors are included in the comparison.

Scalings of Stark widths with electron temperature T_e (Fig. 3) and electron density n_e (Fig. 4) are investigated, and reasonable agreement is found with calculations.

The behavior of the Stark widths along the isoelectronic sequence (Fig. 5) was studied. The results favor no simple scaling law in contradiction to Z^{-2} as suggested by electron-impact theories (e.g., Refs. [5, 6]).

For $Z > 4$, the theoretical approaches [5, 6, 9, 34] give systematically smaller values for the Stark widths as compared with our experiment, the discrepancy becoming larger with increasing ionization stage. This discrepancy increasing with Z could indicate an increasing relative contribution of ion quadrupole broadening at higher temperatures which are necessary to produce the respective ions.

ACKNOWLEDGMENTS

This research was supported by the Sonderforschungsbereich 191 of the DFG. One of us (N.I.U.) wishes to express his gratitude to the Commission of the European Communities for financing his research stay at the Ruhr-Universität Bochum. We would also like to thank H. R. Griem for helpful comments and J. D. Hey for valuable discussions and for performing calculations.

* Permanent address: Institute of Physics, Belgrade, Yugoslavia.

[1] W. L. Wiese and N. Konjević, J. Quant. Spectrosc. Radiat. Transfer **28**, 185 (1982).
[2] R. Kobilarov and N. Konjević, Phys. Rev. A **41**, 6023 (1990).
[3] N. Konjević and W. L. Wiese, J. Phys. Chem. Ref. Data **19**, 1370 (1990).
[4] F. Böttcher, P. Breger, J. D. Hey, and H.-J. Kunze, Phys. Rev. A **38**, 2690 (1988).
[5] H. R. Griem, *Spectral Line Broadening by Plasmas* (Academic, New York, 1974).
[6] M. S. Dimitrijević and N. Konjević, J. Quant. Spectrosc. Radiat. Transfer **24**, 451 (1980).
[7] G. K. Oertel and L. P. Shomo, Astrophys. J. Suppl. Series **16**, 175 (1968).
[8] S. Bashkin and J. O. Stoner, Jr., *Atomic Energy Levels and Grotrian Diagrams* (North-Holland, Amsterdam, 1975), Vols. I and II.
[9] J. D. Hey (private communication).
[10] J. D. Hey and P. Breger, J. Quant. Spectrosc. Radiat. Transfer **24**, 349 (1980); **24**, 427 (1980).
[11] M. Baranger, in *Atomic and Molecular Processes*, edited by D. R. Bates (Academic, New York, 1962).
[12] J. D. Hey and P. Breger, S. Afr. J. Phys. **5**, 111 (1982).
[13] J. D. Hey, A. Gawron, X. J. Xu, P. Breger, and H.-J. Kunze, J. Phys. B **23**, 241 (1990).
[14] K. H. Finken and U. Ackermann, Phys. Lett. **85A**, 278 (1981).
[15] K. H. Finken and U. Ackermann, J. Phys. D **15**, 615 (1982).
[16] H.-J. Kunze, in *Spectral Line Shapes*, edited by R. J. Exton (Deepak, Hampton, 1987), Vol 4.
[17] S. Glenzer, J. Musielok, and H.-J. Kunze, Phys. Rev. A **44**, 1266 (1991).
[18] S. Kawata and S. Minami, Appl. Spectros. **38**, 49 (1984).
[19] A. Gawron, S. Maurmann, F. Böttcher, A. Meckler, and H.-J. Kunze, Phys. Rev. A **38**, 4737 (1988).
[20] D. E. Evans, Plasma Phys. **12**, 573 (1970).
[21] A. W. DeSilva, T. J. Baig, I. Olivares, and H.-J. Kunze, Phys. Fluids B **4**, 458 (1992).
[22] L. Spitzer, Jr., Phys. Rev. **58**, 348 (1940).
[23] H. R. Griem, *Plasma Spectroscopy* (Academic, New York, 1964).
[24] J. E. Dennis, Jr. and D. J. Woods, *New Computing Environments: Microcomputers in Large-Scale Computing*, edited by A. Wouk (SIAM, Philadelphia, 1987), p. 116.
[25] W. L. Wiese, in *Plasma Diagnostic Techniques*, edited by R. H. Huddlestone and S. L. Leonard (Academic, New York, 1965).
[26] A. W. DeSilva and T. J. Baig (private communication).
[27] U. Ackermann, K. H. Finken, and J. Musielok, Phys. Rev. A **31**, 2597 (1985).
[28] M. A. El-Farra and T. P. Hughes, J. Quant. Spectrosc.

Radiat. Transfer **30**, 335 (1983).
[29] P. Bogen, Z. Naturforsch. **27a**, 210 (1972).
[30] S. Djeniže, A. Srećković, M. Milosavljević, O. Labat, M Platiša, and J. Purić, Z. Phys. D **9**, 129 (1988).
[31] N. Konjević and W. L. Wiese, J. Phys. Chem. Ref. Data, **5**, 259 (1976).
[32] N. Konjević, M. S. Dimitrijević, and W. L. Wiese, J. Phys. Chem. Ref. Data, **13**, 649 (1984).
[33] H. R. Griem, Phys. Rev. **165**, 258 (1968).
[34] M. J. Seaton, J. Phys. B **21**, 3033 (1988).